Dynamic Photophysical Properties of Conformationally Distorted Nickel Porphyrins. 1. Nickel(II) Dodecaphenylporphyrin

ARTICLE *in* THE JOURNAL OF PHYSICAL CHEMISTRY · JULY 1996

Impact Factor: 2.78 · DOI: 10.1021/jp960735j

6 AUTHORS, INCLUDING:

Charles Michael Drain
City University of New York - Hunter College
118 PUBLICATIONS **3,961** CITATIONS
SEE PROFILE

Craig Medforth
University of Porto
167 PUBLICATIONS **6,002** CITATIONS
SEE PROFILE

Daniel Nurco
University of California, Davis
56 PUBLICATIONS **1,679** CITATIONS
SEE PROFILE

Article

Dynamic Photophysical Properties of Conformationally Distorted Nickel Porphyrins. 1. Nickel(II) Dodecaphenylporphyrin

Charles Michael Drain, Christine Kirmaier, Craig J. Medforth, Daniel J. Nurco, Kevin M. Smith, and Dewey Holten

J. Phys. Chem., **1996**, 100 (29), 11984-11993• DOI: 10.1021/jp960735j • Publication Date (Web): 18 July 1996

Dynamic Photophysical Properties of Conformationally Distorted Nickel Porphyrins. 1. Nickel(II) Dodecaphenylporphyrin

Charles Michael Drain,[†,§] Christine Kirmaier,[†] Craig J. Medforth,[‡] Daniel J. Nurco,[‡] Kevin M. Smith,[‡] and Dewey Holten*[,†]

Department of Chemistry, Washington University, St. Louis, Missouri 63130, and Department of Chemistry, University of California, Davis, California 95616

Received: March 11, 1996; In Final Form: May 21, 1996[⊗]

Transient absorption measurements with subpicosecond resolution have been performed on nickel(II) dodecaphenylporphyrin (NiDPP), a highly nonplanar tetrapyrrole. Following photoexcitation, NiDPP deactivates by the pathway $(\pi,\pi^*) \rightarrow$ (d,d) $\rightarrow$ ground state, the route proposed previously for planar analogues. However, the (π,π^*) state has now been spectrally and kinetically resolved, and evidence is presented that the deactivation proceeds mainly in the singlet manifold. The lifetime of the $^1(\pi,\pi^*)$ state of NiDPP is about 0.7 ps in all solvents investigated and increases only slightly as the temperature is reduced. The (d,d) state exhibits complex spectral evolution over the following 20 ps or more, which is interpreted in terms of vibrational relaxation and cooling, together with changes in the conformation of the porphyrin macrocycle. The ligand-field excited state decays with a lifetime of about 120 ps in toluene, but this decay time, like the vibrational and conformational dynamics in the (d,d) state, slows considerably in mineral oil and at low temperature. The solvent dependence of the ground-state absorption spectrum combined with the dependence of the excited-state kinetics on detection wavelength, viscosity, and temperature suggests that NiDPP has a number of accessible conformers and that the energies of these conformers and the barriers between them differ with the electronic state. Such conformers probably differ in the type and degree of nonplanar distortion (e.g., saddle or ruffled) and in the orientations and solvent interactions of the phenyl rings. The results presented here for NiDPP, together with previous time-resolved data on metal-free nonplanar porphyrins, suggest that key properties of nonplanar tetrapyrroles include ready access to multiple conformers and a propensity for photoinduced conformational changes. Collectively, the results of spectroscopic studies on nonplanar porphyrins suggest that static and dynamic functional properties of tetrapyrrole cofactors in vivo may be strongly modulated by the steric constraints imposed by a protein matrix.

Introduction

The chemical and photochemical reactivity of metalloporphyrins may be tuned by distortions in the otherwise planar geometry of the porphyrin ligand.[1] Nature accomplishes these distortions of the porphyrin ring in several ways, such as addition of exocyclic rings, reduction in one or more of the pyrrole subunits, axial ligation, and constraints exerted by the surrounding protein.[2,3] The effects on chemical reactivity are nicely illustrated by an enzymatic system in methanogenic bacteria. The final step in methane formation by methanogenic bacteria requires an unusual, highly reduced nickel tetrapyrrole cofactor, F_{430}, to catalyze the reduction of a methyl sulfide to methane and a disulfide.[4] The severe distortion[5] of F_{430} in the enzyme modulates the reactivity since planar nickel porphyrins, such as nickel protoporphyrin IX, are ineffective by themselves or in the enzymatic system, while a non-porphyrin, nonplanar nickel macrocycle also catalyzes the methyl sulfide reduction.[6] There are numerous examples of nonplanar metallotetrapyrroles in a variety of biological systems[7] ranging from photosynthetic reaction centers[3c] to vitamin B_{12}.[3b] Synthetically, these distortions may be accomplished by steric interactions of exo ring substituents such as dodecaaryl or -alkyl substitution.[8] One example is 2,3,5,7,8,10,12,13,15,17,18,20-dodecaphenylporphinatonickel(II), NiDPP (Figure 1), the subject of this article.[9]

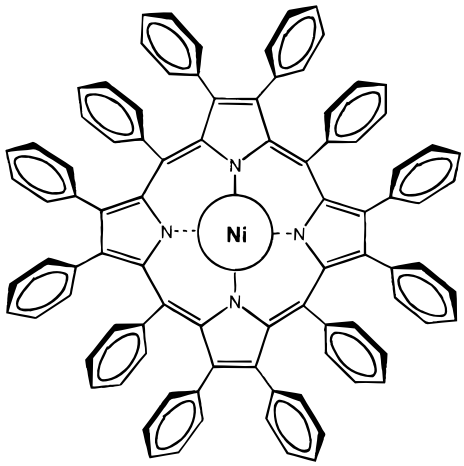

Figure 1. 2,3,5,7,8,10,12,13,15,17,18,20-Dodecaphenylporphyrinatonickel(II) (NiDPP). Calculated structural parameters[8c] for NiDPP: Ni−N bond distance = 1.915 Å, the opposite N−Ni−N bond angle = 163.8°, C−N−N−C dihedral angle = 17°. For square-planar NiTPP these are calculated (and found) to be 1.952 Å (1.948 Å), 180°, and 0.8°, respectively. R_0(Ni−N) = 1.850 and 2.070 Å for low- and high-spin complexes, respectively.[19]

Recent studies of metal-free DPP and other free-base nonplanar porphyrins have demonstrated the significant effects of macrocycle distortion on their photophysical behavior.[10,11] For example, nominally planar complexes such as H_2TPP (TPP is 5,10,15,20-tetraphenylporphyrin) have lowest $^1(\pi,\pi^*)$ excited-state lifetimes of 10−20 ns. The out-of-plane distortions in H_2-

[†] Washington University.
[‡] University of California.
[§] Present address: Department of Chemistry, Hunter College of CUNY, New York, NY 10021.
[⊗] Abstract published in *Advance ACS Abstracts,* July 1, 1996.

S0022-3654(96)00735-6 CCC: $12.00

DPP result in a shortening of the $^1(\pi,\pi^*)$ lifetime to ~800 ps and a corresponding reduction in the yield of fluorescence emission.[11a] Even more dramatically, the ruffled structure resulting from the presence of tertiary butyl groups at the four meso carbons of H_2T(*tert*-butyl)P results in a singlet lifetime of ~20 ps at room temperature that returns to the nanosecond time scale at low temperature.[11b] The perturbed excited-state lifetimes of these nonplanar metal-free porphyrins arise from enhancement of the rates of both internal conversion and intersystem crossing. Additionally, these molecules exhibit a substantial shift between the absorption and fluorescence maxima, indicative of a significant coordinate displacement between the ground and excited electronic state potential energy surfaces. Emerging from these studies and the work described below is the idea that distorted porphyrins may not be locked into one static conformation but may have low energy barriers to other nonplanar conformations. Furthermore, the barriers may be even further altered in the electronic excited state, permitting complex conformational excursions and excited-state dynamical behavior that may be highly dependent on variables such as the detailed substituent pattern on the macrocycle, the temperature, and the medium.

Complex and varied behavior may also be exhibited by the metal derivatives of distorted porphyrins since metalation can result in significant changes in the degree of nonplanarity, conformational flexibility, and electron density distribution of the macrocycle.[8,12] Recent crystallographic data[13a] and the results of molecular modeling studies[13b] support the suggestion that nickel(II) dodecaphenylporphyrins can access a range of saddle and ruffled conformations in the ground electronic state. Out-of-plane distortions may lead to significant interactions between orbitals that are essentially orthogonal in the planar molecules, as evidenced by an increase in antiferromagnetic coupling between the unpaired electrons of the porphyrin π-cation radical with the paramagnetic metal ion in Cu(II)-OETPP.[9,12d] Nickel(II) porphyrins are especially useful for investigating the conformational properties of the macrocycle.[14,15] The small ionic radius of 0.69 Å[16] for nickel(II) tends to pull the pyrrole nitrogens inward and contract the core, resulting in small deformations of porphyrins normally considered planar, such as NiOEP.[9,14]

Nickel(II) porphyrins have rich photophysical behavior that can be exploited to probe the relationships among both static and dynamic conformational, electronic, and vibrational properties. These molecules are nonluminescent ($\phi < 10^{-5}$),[17] making them especially amenable to Raman studies.[14a,15a,b,18] Nickel(II) porphyrins have a d^8 metal electronic configuration, so in the absence of axial ligands the d_{z^2} orbital is the highest filled metal orbital and the $d_{x^2-y^2}$ orbital is empty. The lack of luminescence, together with the results of extended Hückel calculations, led to the proposal that the normally emissive (π,π^*) excited states of the macrocycle deactivate rapidly via low-energy singlet and/or triplet forms of the $(d_{z^2},d_{x^2-y^2})$ excited state, henceforth referred to as the (d,d) state.[17] Indeed, ultrafast absorption measurements of common nickel porphyrins such as NiOEP and NiTPP have revealed that a (d,d) state forms within <1 ps,[19] followed by deactivation to the ground state in 200−500 ps.[20−22] However, these studies have neither kinetically resolved the $^1(\pi,\pi^*)$ excited state nor clearly demonstrated whether deactivation of this state to the ground state proceeds exclusively through the ^{1}(d,d) state or involves intersystem crossing followed by decay of the ^{3}(d,d) state. These routes are illustrated in Figure 2.

An intriguing aspect of the photophysics of nickel porphyrins is that they display photoinduced transient nuclear dynamics. For example, the transient optical bands of the (d,d) excited

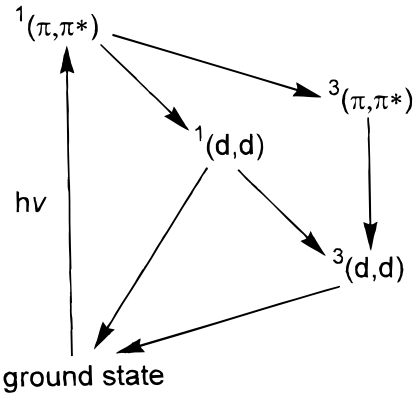

Figure 2. Jablonski diagram of possible excited-state decay pathways that have been considered for four-coordinate nickel(II) porphyrins.

state in noncoordinating media narrow and blue-shift with wavelength-dependent kinetics on the 5−25 ps time scale.[19] This complex spectral evolution has been modeled and interpreted as arising from the transient presence of excess vibrational energy, resulting from the rapid (<1 ps) radiationless decay from the (π,π^*) excited state to the lower-energy (d,d) excited state. In this model, the excess energy dissipates on the 5−25 ps time scale as the porphyrin "cools" by flow of the vibrational energy into the solvent. This interpretation is supported by the observation of similar behavior for a variety of metal-containing and free-base porphyrin complexes following an ultrafast radiationless decay process.[19,23] Additionally, similar behavior has been observed on this time scale and attributed to vibrational cooling for a number of other large molecules.[24] Alternatively, the spectral evolution observed on the 5−25 ps time scale for nickel protoporphyrin(IX) dimethyl ester has been attributed to the evolution of the (d,d) excited state from a ruffled to planar conformation.[18c] Core expansion or other structural changes are expected in the (d,d) excited state compared to the ground state in order to relieve the repulsion between the $d_{x^2-y^2}$ electron and the lone-pair electrons of the central nitrogen atoms.

However, conformational processes per se cannot account for the blue shifts occurring on the 5−25 ps time scale following formation of the $(d_{z^2},d_{x^2-y^2})$ excited state of four-coordinate nickel porphyrins, since similar transient blue shifts have been observed following formation of the $(d_{z^2})^2$ excited state of six-coordinate complexes such as NiTPP(piperidine)$_2$.[23b] The four- and six-coordinate complexes would be expected to show opposing shifts in the planarity of the macrocycle and thus should give transient spectral shifts in the opposite direction. On the other hand, the structural excursions in the excited electronic state may be more complex than a simple conversion between a planar and specific nonplanar conformer and may include several accessible conformers and changes in the interactions between the macrocycle and the solvent. Additionally, vibrational relaxation and transient changes in mean structure are inevitably intertwined if the potential energy surfaces for the electronic states involved are anharmonic. This might be expected to be the case for the nickel porphyrins, since low-frequency out-of-plane deformational motions accompanying the photoinduced conformational change probably have relatively anharmonic potentials. Such low-frequency modes are expected to play an important intermediary role in the vibrational cooling process wherein the excess vibrational energy moves from the high-energy vibrations through lower-energy modes and into the medium. Anharmonic effects also may be important in defining the perturbations to the optical spectra that accompany the presence of excess vibrational energy.[19c] For all of the reasons outlined above, nonplanar nickel porphyrins such as NiDPP provide a unique opportunity to address

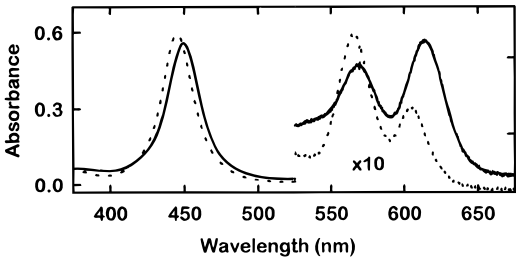

Figure 3. Ground-state spectra of NiDPP in methylcyclohexane (- - -) and toluene (—) at the same concentration and experimental conditions.

fundamental issues concerning vibrational relaxation and conformational dynamics in large molecules, as well as the mechanisms by which different nonplanar distortions of the porphyrin macrocycle can lead to altered photophysical properties. These structurally distorted molecules are also ideal for addressing the key unresolved issues concerning the radiationless decay pathways in this widely studied class of metalloporphyrins. Therefore, we have embarked on an extensive program of study of the excited state spectral and dynamic behavior of nonplanar nickel porphyrins using transient absorption spectroscopy with ~150 fs time resolution. During the course of this study we have investigated some 25 complexes, in a variety of solvents, as a function of temperature, and using a number of excitation wavelengths in the visible and near-UV. NiDPP displays the most complex excited-state behavior of any of the compounds studied, and so we have investigated this molecule in considerable detail. Here we present the results of this study. The results and discussion herein lay the groundwork for presentation of our findings on the whole series of complexes and, most importantly, illustrate how the complex, interrelated affects of nonplanarity and vibrational/conformational relaxation impart rich electronic and photophysical properties to these molecules and, by implication, to tetrapyrrole active sites in biological systems.

Experimental Section

NiDPP was prepared as described previously.[8] Spectral grade solvents were used for all studies. Ground state absorption spectra were acquired on a Cary Bio-1 spectrometer. Transient absorption measurements utilized either 150-fs 582-nm excitation flashes from an amplified synchronously pumped dye laser system (Spectra Physics) or ~120-fs blue pulses obtained by frequency doubling the output of a regeneratively amplified mode-locked Ti:sapphire system (Spectra Physics and Positive Light). In either case, absorption changes were measured using a white-light pulse of ~150-fs duration and two-dimensional detection, as described previously.[19] Low-temperature measurements utilized an Oxford Instruments cryostat.

Results

Ground Electronic State Absorption Spectra. The ground electronic state absorption spectrum of NiDPP is quite solvent dependent, even in noncoordinating media such as toluene and methylcyclohexane (Figure 3 and Table 1). In contrast, the ground-state absorption spectra of common nickel porphyrins such as NiTPP are essentially unchanged among these solvents (Table 1). In general, both the strong near-UV Soret and the weaker visible Q bands of NiDPP are red-shifted in aromatic solvents compared to aliphatic media, and the ratio of the two Q bands is reversed. The absorption bands of NiDPP are significantly broader[8] (about 1.5 times) than the spectral features of NiTPP. The NiDPP spectrum in mineral oil is intermediate between those found in the aromatic vs aliphatic solvents, both in the positions of the absorption bands and in the approximately

TABLE 1: Ground-State Spectral Properties[a]

porphyrin	solvent	Soret (B)	Q(1,0)	Q(0,0)
NiDPP	toluene	449 (12)	570 (1)	614 (1.2)
	mesitylene	450 (15)	569 (1)	615 (1.4)
	methylcyclohexane	445 (10)	565 (1)	605 (0.53)
	3-methylpentane	445 (13)	567 (1)	610 (0.93)
	mineral oil	447 (14)	564 (1)	609 (0.93)
NiTPP	toluene	415 (14)	527 (1)	560 (<0.1)[b]
	methylcyclohexane	414 (14)	527 (1)	560 (<0.1)[b]
NiOETPP	toluene	434 (16)	554 (1)	591 (0.86)
	methylcyclohexane	434 (16)	554 (1)	591 (0.82)

[a] Wavelengths are in nanometers. The values in parentheses are the peak amplitudes relative to the Q(1,0) band. See ref 9 for abbreviations of the porphyrins. [b] This feature is a shoulder on the Q(1,0) band.

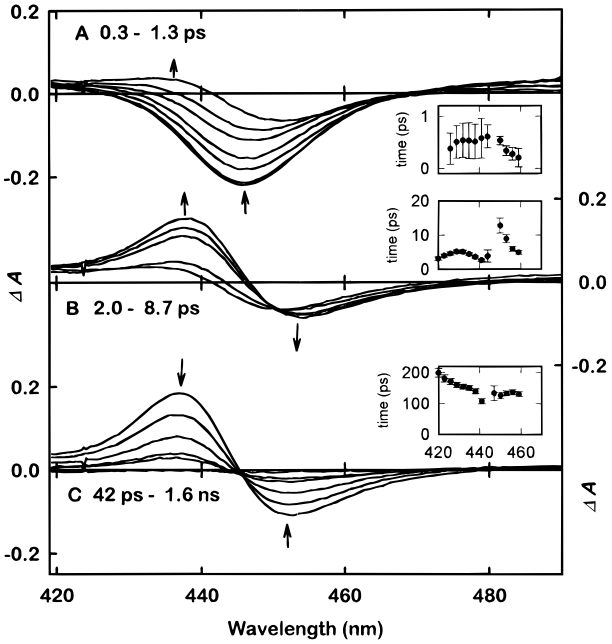

Figure 4. Transient absorption difference spectra in the Soret region of NiDPP in methylcyclohexane acquired following a 150-fs excitation pulse at 582 nm: (a) the first 1.3 ps, (B) 2.0−8.7 ps, and (C) 42 ps to 1.6 ns. The insets show wavelength variation of the time constants derived from the kinetic data such as shown in Figure 5.

equal intensities of the two Q bands. In 2-methyltetrahydrofuran, the Soret band shifts from 447 to 452 nm and decreases in width by about 60% as the temperature is lowered from 298 to 78 K. This temperature dependence is not appreciably different than for NiTPP and other common porphyrins.

Time-Resolved Absorption Difference Spectra. Near-UV and visible-region transient absorption changes and kinetic data with ~150-fs time resolution were acquired for NiDPP in a number of solvents and at various temperatures, using several different excitation wavelengths. In each case, the time evolution of the spectra is quite complex and reveals three or four kinetic components, with time constants ranging from the subpicosecond domain to the nanosecond domain before complete ground-state recovery is observed. Even this is a minimal description since on some time scales and in some wavelength regions the apparent time constants vary with detection wavelength, indicating that the associated spectral evolution rigorously reflects either the presence of more exponential components or distributed kinetics. However, the signal-to-noise ratio of the data is not sufficient to distinguish these possibilities. The photophysical behavior has both notable similarities and striking differences in various solvents, and so the results in the different media are presented separately.

Methylcyclohexane. Figure 4 shows time-resolved absorption data in the Soret region for NiDPP in methylcyclohexane

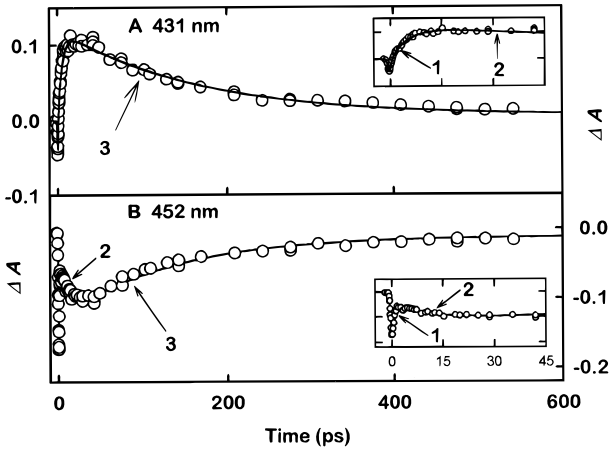

Figure 5. Representative kinetic data and the fits, to a three-exponential function, of the time evolution of the absorption difference of NiDPP in methylcyclohexane from Figure 4: (A) transient absorption and (B) ground-state bleaching. The arrows indicate the three kinetic phases and the alternating signs of the corresponding preexponential factors at these wavelengths.

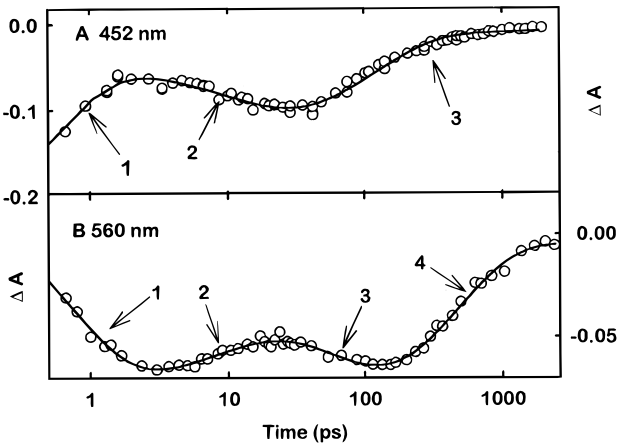

Figure 6. Representative kinetic data and fits for NiDPP in methylcyclohexane plotted in log time to illustrate the complex spectral evolution at (A) 452 and (B) 560 nm. The arrows indicate the different kinetic phases and the alternating signs of the corresponding preexponential factors at these wavelengths.

at 298 K, acquired using 150-fs excitation flashes at 582 nm. Over the first 2 ps after excitation, the prominent bleaching of the ground-state Soret band decreases while an excited-state absorption develops to the blue (Figure 4A). As will become apparent, the small amplitude of the spectrum at 1.3 ps (top spectrum in Figure 4A) compared to spectra at earlier and later times must arise from substantial overlap of opposing Soret ground-state bleaching and excited-state absorption. Over the next 20 ps or so, the difference spectrum continues to evolve into one having a derivative-like shape (Figure 4B). Over the following several hundred picoseconds, the derivative-shaped spectrum decays uniformly to the baseline, reflecting complete ground-state recovery, with an apparent isosbestic point near 445 nm (Figure 4C).

Representative Soret-region kinetic data are shown in Figures 5 and 6A, the latter plotting ΔA vs log time. Visual inspection of these data, like the spectral data of Figure 4, indicates that there are three domains of the time evolution, and the kinetic data were analyzed using a triple-exponential function. The insets in Figure 4 summarize the wavelength variation of the time constants derived from the analysis. The three phases have average time constants of 0.6, 6, and 150 ps over the 420−460 nm region (Table 2). Although the value of the first time constant is essentially wavelength independent, the second component changes by about a factor of 2 across the red edge of the Soret region and third phase approaches 200 ps on the blue edge of the spectrum.

Typical data through the ground-state Q bands and to the red, acquired using 120-fs 425-nm excitation flashes, are shown in Figure 7. There are four components to the time evolution of these spectral changes, which are most apparent from the absorption changes in the Q(1,0) bleaching near 560 nm. In this region, the direction of the time evolution of ΔA changes sign in each of the four domains (Figures 6B and 8A). During the first several picoseconds, there is a fairly substantial, uniform decrease in a broad transient absorption that tails from the Soret region to past 650 nm, broken by bleachings in the Q bands (Figure 7A). Like the Soret region, more subtle readjustments of the spectrum occurs during the next 20 ps (Figure 7B). Subtle spectral changes also occur over the next ∼200 ps, and ΔA changes direction with time in both bleachings opposite to the spectral evolution on the 20-ps time scale (Figure 7C). Finally, the resulting spectrum decays uniformly to $\Delta A = 0$ with apparent isosbestic points flanking both ground-state bleachings (Figure 7D).

The average time constants of 0.7 and 7 ps for the first two components in the Q-band region are comparable to those of the first two components found in the Soret data. The third and fourth components in the visible region have average values of 130 and 410 ps and correspond to absorption changes in the opposite direction over most of the spectral region shown (see Figures 6B, 7C,D, and 8). An exception is in the Q(0,0) bleaching near 610 nm, where both components apparently represent decay of the bleaching, are not readily separated, and are analyzed adequately with a single exponential having an intermediate time constant of 160 ps (Figure 8B). This observation raises the possibility that the average time constant of 150 ps found for the third, slowest component in the Soret region reflects a composition of two components having substantially overlapping spectral changes and time constants similar to the third and fourth components in the Q-band data.

Transient absorption and kinetic data were also taken in the Soret region for NiDPP in methylcyclohexane at low temperature, both above and below the 146 K freezing point of the solvent (Table 2). The average time constants of the first two phases increase from approximately 0.6 to 3 ps and 6 to 30 ps, respectively, as the temperature is reduced from 298 to 230 K, and essentially the same values are obtained in the frozen sample at 78 K. The time constant of the third, slowest phase progressively increases as the temperature is reduced, from ∼150 ps at 298 K to over 3 ns at 78 K. The data at 298, 230, and 200 K yield an estimate of 3 kcal/mole for the activation energy of this ground-state recovery process.

Toluene. The Soret-region transient absorption and kinetic data for NiDPP in toluene at 298 K (not shown) are very similar to the data obtained in methylcyclohexane (Figure 4 and Table 2). Similar kinetic data were found in the Q bands, using either 415-, 425-, 430-, or 582-nm excitation flashes. The average time constant of the ground-state recovery phase lengthens from 120 ps at 298 K to 350 ps at 200 K (which is slightly above the 178 K freezing point of the solvent), as measured in the Soret region. The value at 200 K is appreciably faster than the 1.7-ns time constant obtained in methylcyclohexane at this temperature. From the lifetimes at 298 and 200 K, a rough estimate of 2 kcal/mol is obtained for the activation energy of the slow kinetic phase in toluene. To elucidate whether intersystem crossing is involved in one or more of the kinetic steps, 10% by volume (1.6 M) methyl iodide in toluene was used as the solvent and resulted in only slightly shorter average time constants (Table 2).

TABLE 2: Summary of Kinetic Data

solvent[a]	temp (K)	λ_{exc} (nm)	region[b]	$(\pi,\pi^*) \rightarrow$ (d,d) (ps)	(d,d) relaxn (ps)[c]	(d,d) $\rightarrow$ ground (ns)[d]
NiDPP						
MCH	298	582	B	0.6 ± 0.2	6 ± 3	0.15 ± 0.03
MCH	298	425	Q	0.9 ± 0.3	7 ± 3	0.13 ± 0.06[e]
						0.41 ± 0.05
MCH	230	582	B	3 ± 1	33 ± 7	0.46 ± 0.03
MCH	200	582	B			1.7 ± 0.3
MCH	78	582	B	3 ± 1	31 ± 7	>3
Tol	298	582	B	0.6 ± 0.1	4 ± 1	0.12 ± 0.2
Tol	298	582	Q		5 ± 1	0.06 ± 0.02[e]
						0.11 ± 0.02
Tol	298	415	Q	0.5 ± 0.1	9 ± 3	0.15 ± 0.02
Tol	298	425	Q	0.7 ± 0.3	10 ± 6	0.08 ± 0.03[e]
						0.14 ± 0.04
Tol	298	430	Q	0.8 ± 0.2	11 ± 6	0.13 ± 0.02
Tol	200	582	B	2 ± 1	34 ± 8	0.31 ± 0.04
Tol + MeI	298	582	B	0.4 ± 0.1	4 ± 1	0.10 ± 0.02
min oil	298	582	B	0.7 ± 0.2	*f*	1.7 ± 0.3[g]
min oil	298	425	Q	0.7 ± 0.2	*f*	1.2 ± 0.2
NiPPDME						
Tol	298	582	B	0.4 ± 0.1	7 ± 4	0.41 ± 0.09

[a] The solvents are MCH = methylcyclohexane, Tol = toluene, Tol + MeI = toluene + 10% methyl iodide by volume, min oil = mineral oil. [b] Detection regions: B is the Soret region (400−500 nm) and Q is the Q-band region (500−700 nm). [c] The time constant attributed to vibrational/conformational dynamics in the (d,d) excited state normally shows a variation with detection wavelength similar to that seen in Figure 3b (i.e., the time constant decreases with increasing wavelength across the red side of the spectral feature. The reported value is the average (±standard deviation). [d] The deactivation of the (d,d) state often shows a variation with detection wavelength near one or both edges of the spectral region investigated, similar to that seen in Figure 4C. The reported value is the average value (±standard deviation). [e] This component probably reflects, at least in part, the relaxation process(es) in the (d,d) excited state and not simply deactivation of the (d,d) state. [f] For NiDPP in mineral oil, several components appear to contribute to the relaxation in the (d,d) excited state, on the time scales of several to tens of picoseconds and one to several hundred picoseconds. [g] The deactivation of the (d,d) state of NiDPP in mineral oil appears to have additional component with a time constant >3 ns.

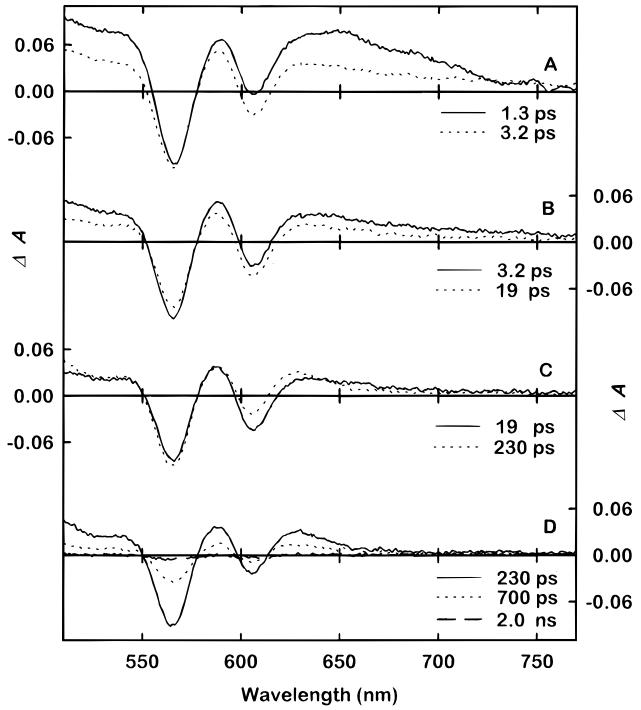

Figure 7. Transient absorption difference spectra in the Q-band region of NiDPP in methylcyclohexane following a 120-fs excitation pulse at 425 nm.

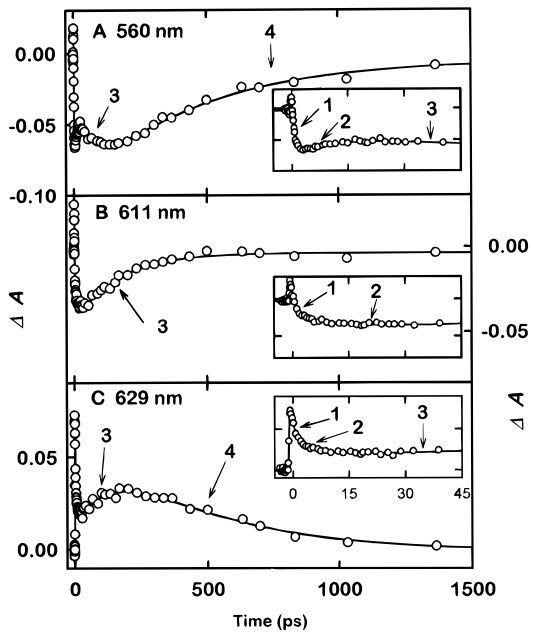

Figure 8. Representative kinetic data and fits, to a four-exponential function, of the time evolution of the absorption difference spectra of NiDPP in methylcyclohexane from Figure 7. The arrows indicate the four kinetic phases and the alternating signs of the prexponential for all the phases at (A) 560 and (C) 629 nm. At 611 nm (B) the two slowest phases both represent decay of the Q(1,0) bleaching, and thus only three components are resolved at this wavelength.

Mineral Oil. To probe the effect of viscosity on the excited-state decay kinetics, data were acquired for NiDPP in mineral oil. The transient data in the Soret region, acquired using 582 nm excitation, revealed four stages to the time evolution (Figure 9). The earliest phases have very similar spectral evolution to those observed in methylcyclohexane (compare Figure 9A with 4A and Figure 9B with 4B). The 0.7-ps time constant of the initial phase is essentially the same as that observed in toluene and methylcyclohexane. The 10−20 ps time constant of the second phase appears to be slightly longer than found in the less viscous solvents, and there may be additional, slower contributions as well. Subsequently, there is a period of well over 100 ps when the spectral shape remains essentially constant (Figure 9C). The derivative-shaped difference spectrum then collapses to near $\Delta A = 0$ with an average value of ~1.7 ns

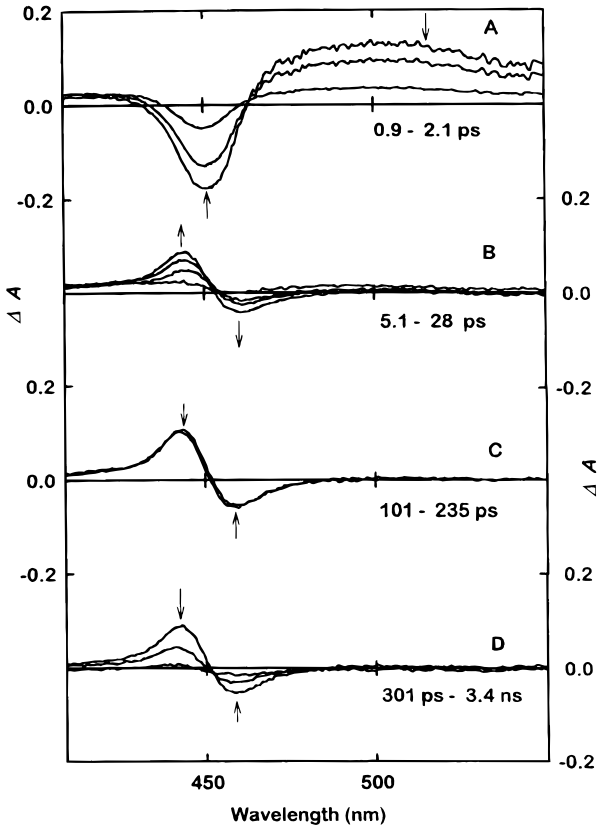

Figure 9. Transient absorption difference spectra in the Soret region of NiDPP in mineral oil at the noted times following excitation at 582 nm.

(Figure 9D). This ground-state recovery phase may actually be more complex than single exponential, since a small fraction of the decay extends past the ~3.4 ns time limit of measurements. Nonetheless, it is clear that the slowest kinetic phase, reflecting ground-state recovery, in mineral oil is significantly slower than in methylcyclohexane or toluene (Table 2). Similar kinetics were found in the Q-band region.

Soret-Region Data for NiPPDME in Toluene. We studied nickel protoporphyrin(IX) dimethyl ester in order to facilitate comparisons between the results obtained here on NiDPP and those found previously for common nickel porphyrins such as NiPPDME, NiOEP, and NiTPP. Representative data on NiPPDME in toluene using 150-fs 582-nm excitation flashes are shown in Figure 10. There is a fast component having a time constant of ~0.4 ps. This value is slightly shorter than the decay time of the fast component of NiDPP, but the evolution of the Soret-region spectrum on this time scale for NiPPDME is much less dramatic (compare Figures 10A and 4A). Subsequently, a derivative-shaped absorption spectrum develops with an average time constant of ~6 ps (Figure 11B). During this time, the peak of the transient absorption slightly shifts to the blue, with no isosbestic point apparent in the spectrum. The 46-ps spectrum has the transient absorption red-shifted from the ground-state bleaching, which is just the opposite of the spectrum observed on this time scale for NiDPP, in which the transient absorption is blue shifted from the bleaching (compare Figures 10B and 4B). Subsequently, the derivative-like spectrum decays to the baseline with an average time constant of about 400 ps, with an apparent isosbestic point near 400 nm (Figure 10C). The observation of isosbestic behavior as the absorption and bleaching decay to $\Delta A = 0$ is similar to the behavior observed for NiDPP in toluene (compare Figures 10C and 4C), although the decay time is longer for NiPPDME (Table 2).

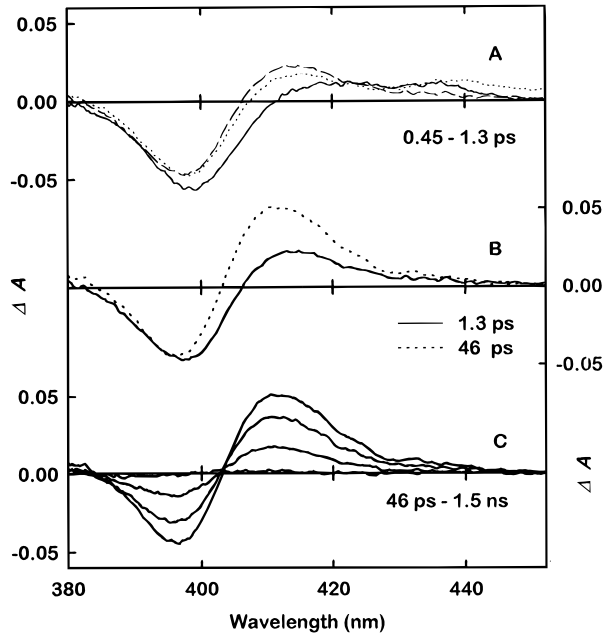

Figure 10. Transient absorption difference spectra in the Soret region of NiPPDME in toluene obtained following excitation at 582 nm.

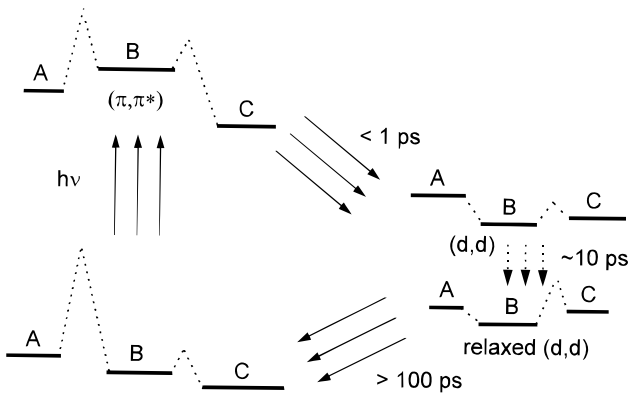

Figure 11. Scheme illustrating that each electronic state may have multiple accessible conformers (denoted A, B, and C) having different zero-point energies and barriers.

Discussion

Ground Electronic State Absorption Spectra. Some of the differences between the ground-state absorption spectrum of NiDPP and planar porphyrins such as NiTPP have been discussed previously.[8] The most prominent change in the spectrum of NiDPP compared to NiTPP is that the Soret and Q bands are considerably red-shifted, even in noncoordinating media (Table 1). Such red-shifts appear to be characteristic of nonplanar porphyrins.[2b,8,11,12,15] INDO/CI calculations suggest that the shifts in the $\pi \rightarrow \pi^*$ transitions are due primarily to destabilization of the porphyrin $a_{1u}(\pi)$ and $a_{2u}(\pi)$ HOMOs, with little change in the $e_g(\pi^*)$ LUMOs.[8b] An upshift in the energies of the HOMOs is consistent with the finding that NiDPP is easier to oxidize than NiTPP.[25] There are undoubtedly both structural and electronic contributions of the eight β-pyrrole phenyl groups (Figure 1) to the differences in the HOMO energies of NiDPP versus NiTPP. These contributions include an inductive effect that raises the energy of the $a_{1u}(\pi)$ HOMO, an orbital that places considerable electron density at the β-pyrrole carbons. The out-of-place distortions in NiDPP will also affect the interaction of the metal d_{z^2} and $d_{x^2-y^2}$ orbitals with the $a_{2u}(\pi)$ HOMO, an orbital that places electron density mainly on the central nitrogens and the meso carbons.

Another noteworthy difference between the ground-state spectra of NiTPP and NiDPP is that the Q(0,0) band is virtually absent in the former, whereas this band is well resolved for the latter. For NiDPP in toluene, the Q(0,0) band is even more intense than the Q(1,0) band, as it is in NiOEP (Figure 3 and Table 1). According to the four-orbital model, the intensity of the Q(0,0) band is directly related to the energy separation between the nearly degenerate (a_{1u},e_g) and (a_{2u},e_g) one-electron excited configurations.[17b] The increased intensity of the Q(0,0) band in NiDPP implies that the presence of phenyl substituents at the β-carbons causes a larger difference in the energies of $a_{1u}(\pi)$ and $a_{2u}(\pi)$ HOMOs than in NiTPP, corresponding to a difference in the ground-state electron density distributions in the two macrocycles. Similarly, there is a difference in the electron spin distributions in the respective cation radicals.[12]

The solvent can further modulate the effects of the peripheral phenyl groups on the structure and electron density distributions in NiDPP. The Soret and Q bands are red-shifted, and the intensity of Q(0,0) relative to Q(1,0) is increased in aromatic solvents compared to aliphatic media (Figure 3). These effects suggest that π-stacking of the solvent and the phenyl substituents directly affects the electronic perturbations of the phenyl groups on the macrocycle electronic distribution, alters the out-of-plane distortions of the macrocycle, or causes rotation of some of the phenyl groups and a change in their conjugation with the macrocycle. The smaller solvent dependence of the spectra of both NiTPP and NiOETPP supports this point of view (Table 1). A distribution of effects involving the precise solvent interactions and orientations of the 12 phenyl groups may contribute to the increased widths of the absorption bands of NiDPP compared to simpler complexes such as NiTPP.

Collectively, these data suggest that NiDPP in the electronic ground state may be able to access multiple conformations. These conformers would involve variations in the basic macrocycle structures (saddled, ruffled, domed, planar, etc.) and/or different orientations and solvent interactions of the peripheral phenyl substitutents. We hypothesize below that conformational excursions may be even more facile in the (π,π*) and (d,d) electronic excited states due to differences in the relative energies of the conformers and the energy barriers between them, as is illustrated schematically in Figure 11.

Characterization of the Lowest $^1(\pi,\pi^*)$ Excited State. The excited-state dynamics begin by formation of the lowest $^1(\pi,\pi^*)$ excited state. This state is produced directly by photon absorption in the visible Q bands or by rapid radiationless deactivation following excitation in the near-UV Soret region. Previous studies of common nickel porphyrins such as NiTPP, NiOEP, and NiPPDME have not spectrally or kinetically resolved the $^1(\pi,\pi^*)$ state. Our new studies on NiDPP and NiPPDME using ~150-fs flashes clearly resolve a transient that evolves into the (d,d) state with a subpicosecond time constant. The broad, featureless transient absorption and the lack of one or more peaks between 750 and 950 nm (Figures 4, 7, and 10) are evidence that the early-time spectra are due to the lowest $^1(\pi,\pi^*)$ state rather than a $^3(\pi,\pi^*)$ state.[19] A detail of the $^1(\pi,\pi^*)$ spectra relevant to analysis of the spectra at later times is the apparent absence of the expected excited-state Soret band. However, close examination of the time evolution of the spectra suggests that this band is present but is not cleanly resolved in the difference spectra because of substantial overlap and cancellation with the opposing bleaching of the ground-state Soret band.[26]

Decay of the $^1(\pi,\pi^*)$ Excited State. The transient spectra ascribed to $^1(\pi,\pi^*)$ for NiDPP in methylcyclohexane, toluene, and mineral oil decay with an average time constant of about 0.7 ps at 298 K. The decay time increases modestly to ~3 ps as the temperature is reduced to 200 K (Table 2). The data set indicates that the $^1(\pi,\pi^*)$ lifetime largely reflects formation of the (d,d) excited state, without significant deactivation to the ground state or $^3(\pi,\pi^*)$ formation (see Figure 2).

Several factors suggest that the intersystem crossing pathway is not significant. Subpicosecond intersystem crossing from $^1(\pi,\pi^*)$ to $^3(\pi,\pi^*)$ is not expected for a porphyrin containing a first-row diamagnetic metal ion, due to insufficient spin−orbit coupling and an absence of mixing involving unpaired metal and ring electrons. The $^1(\pi,\pi^*)$ lifetime is not significantly perturbed by addition of methyl iodide to the NiDPP solutions (Table 2) or by octabromination of the macrocycle.[27] As noted above, there is also no evidence for $^3(\pi,\pi^*)$, based on the lack of near-infrared absorptions.

Ground-state recovery also does not appear to be a primary decay pathway for the $^1(\pi,\pi^*)$ state, although this process may occur to some degree. The strongest evidence for this conclusion comes from the observation that the extent of bleaching in the ground-state Q bands does not decrease substantially during the ~0.7 ps $^1(\pi,\pi^*)$ lifetime. The lack of appreciable bleaching decay can be seen by comparing the magnitudes of the troughs referenced to the broad positive absorption in the solid and dashed spectra in Figure 7A. If we assume that there are no sharp absorptions at the same wavelengths as the bleachings in this region (or, if there are, that the amplitudes are comparable in the states contributing the spectra during the first picosecond or so), then Q-band data such as those shown in Figure 7A suggest that <30% of the decay of the $^1(\pi,\pi^*)$ state of NiDPP is due to internal conversion to the ground state. It is more difficult to assess the relative importance of the $^1(\pi,\pi^*)$ decay pathways from the data in the blue region due to substantial overlap of opposing absorption changes.[28] Overall, the data are most consistent with the idea that the major pathway involved in the subpicosecond decay of the $^1(\pi,\pi^*)$ state of NiDPP is formation of the ^{1}(d,d) excited state.[20]

Characterization of the (d,d) Excited State. The transient optical data suggest that the ligand-field excited forms directly from $^1(\pi,\pi^*)$ state and, thus, is the ^{1}(d,d) state. The ^{1}(d,d) state then continues to evolve over the next 10 ps or so, a phenomenon we will attribute to conformational/vibrational relaxation (Figure 11). In general, one expects the spectrum of metalloporphyrin (d,d) state to exhibit derivative-shaped absorption changes since the porphyrin π-system has returned to its ground-state electronic configuration. Thus, the absorption spectrum of the (d,d) states should be dominated by the same (π,π*) transitions governing the spectrum of the ground electronic state of the complex but shifted in energy and perhaps intensity due to the new metal electronic configuration. This behavior is realized for the nominally planar complexes investigated previously, such as NiTPP, NiOEP, and NiPPDME, as well as for the highly nonplanar porphyrins such as NiDPP studied here. However, unlike the spectra for the $^1(\pi,\pi^*)$ state, the spectra of the ^{1}(d,d) excited state differ substantially for the two classes of nickel porphyrins.

The (d,d) spectra for the planar compounds all have transient absorption bands immediately to the *red* of the bleachings in the ground state Soret and Q bands (see spectra at 46 ps and longer for NiPPDME in Figure 10B,C). In stark contrast, the excited-state Soret band of NiDPP lies to the *blue* of the ground-state Soret bleaching (Figure 4A). This difference in behavior is independent of solvent and temperature. A blue-shifted Soret band in the (d,d) excited state is also observed for NiT(*tert*-butyl)P, a molecule that has a substantially ruffled structure.[30] These observations strongly suggest that the switched relative positions of the Soret bands in the ground and (d,d) excited

states of the two classes have structural origins, although there are no doubt electronic contributions as well.

Ultimately, the shifted excited state versus ground state Soret bands for both classes must be connected to some extent with the population of the $d_{x^2-y^2}$ orbital in the ligand-field excited state. Population of this orbital and increased repulsion with the ring a_{2u} HOMO will cause a shift in the HOMO−LUMO gap and the (π,π^*) transition energies. This effect will be altered to some degree and perhaps reversed by structural changes that reduce this electron repulsion. In this context, the blue-shift in the transient Soret band of the nonplanar porphyrins relative to the ground state of these complexes may be most easily explained if a less-distorted geometry is assumed in the ligand-field excited state. This interpretation would be consistent with the observations that the ground-state Soret bands of the planar nickel porphyrins lie to shorter wavelengths that those of the distorted analogues. Furthermore, the core size is expected to be larger the more planar the macrocycle, relieving electronic replusion between the metal $d_{x^2-y^2}$ and ring a_{2u} electrons. However, this is but one possibility. There are no doubt other types of distortions that would relieve the electronic repulsion without increasing macrocycle planarity. The elucidation of the principal effects that give rise to the dramatic difference in (d,d) spectra of the planar and nonplanar porphyrins will require further work. Nonetheless, the observations strongly suggest that the opposing behavior for the two classes must be inevitably linked to the differences in ground-state structures and probably the excited-state structures as well.

Vibrational/Conformational Dynamics in the (d,d) Excited State. For both NiDPP and planar analogues such as NiPPDME, the full structural and electronic consequences of the formation of the ^{1}(d,d) excited state are not manifest until at least 15 ps after its formation from $^1(\pi,\pi^*)$. At earlier times, the transient Soret and Q bands of the ligand-field excited state appear to be asymmetrically shifted and broadened to longer wavelengths, and the evolution to the spectrum observed at longer times for the ^{1}(d,d) state is complex. This behavior has been observed previously and analyzed in detail for planar porphyrins such as NiTPP, NiOEP, and NiPPDME. The data have been taken to reflect the presence of the considerable (probably over 0.5 eV) vibrational energy deposited in the porphyrin from the ultrafast $^1(\pi,\pi^*) \rightarrow {}^1$(d,d) nonradiative decay process.[19] The overall process by which the energy is redistributed within the porphyrin and flows into the medium apparently requires several to tens of picoseconds.

Some representative spectral data for NiPPDME are shown in Figure 10B. The transient Soret band in the 1.3-ps spectrum has a net red-shift compared to the spectrum at longer times, and the evolution of the spectrum is characterized by the absence of isosbestic points. Additionally, there is a wavelength dependence of the apparent time constant, which increases from a few picoseconds on the red edge of the transient absorption near 430 nm to over 10 ps at 410 nm, nearer to the positive ΔA maximum in the spectrum. The average value is about 7 ps. The lack of isosbestic behavior and the wavelength dependence of the kinetics suggests that the inherent kinetics at any wavelength are more complex than described by the simple single-exponential function used to fit the data on this time scale. This complexity would arise because the process involves changing populations of a distribution of vibrational levels. As noted in the Introduction, similar spectral behavior has been observed for a number of porphyrin complexes[19,23] and other large molecules[24] and ascribed largely to vibrational cooling. The wavelength dependence of the time constant and the lack of isosbestic behavior also indicates that the ∼7 ps process does not reflect a simple conversion of one electronic state to another, such as intersystem crossing from $^1(\pi,\pi^*)$ to $^3(\pi,\pi^*)$.[19a]

We propose that the similarly complex spectral evolution observed for NiDPP in toluene, methylcyclohexane, and mineral oil is also due, at least in part, to vibrational relaxation. Since in this case the Soret absorption band of the relaxed (d,d) excited state is blue-shifted from the ground-state bleaching, the characteristic evolution of the enhanced and broadened red side of this transient absorption shows up during the first 10−20 ps as an increasing bleaching amplitude and a small blue-shifting of the peak of the positive absorption (Figure 4B). Again, the apparent time constant increases from longer to shorter wavelengths on the red edge of this region, with an average time constant of about 7 ps (Figure 4B inset). The spectrum in the Q-band region also evolves on this time scale, but with more subtle absorption changes (Figure 7B).

In addition to the vibrational relaxation that must inevitably follow the $^1(\pi,\pi^*) \rightarrow {}^1$(d,d) decay process, this electronic transition is also expected to engender a change in the equilibrium geometry of the nickel porphyrin. As noted above, a change in geometry is minimally expected to relieve the increased electron repulsion arising from population of the metal $d_{x^2-y^2}$ orbital. Additionally, on the basis of previous work on nonplanar metal-free porphyrins, one might also expect that the initial excitation of the $^1(\pi,\pi^*)$ excited state itself may induce a structural shift from the ground-state configuration(s).[11] *Thus the ground, $^1(\pi,\pi^*)$, and ^{1}(d,d) states may be structurally different.* This situation may be especially complicated for NiDPP by the low barriers that appear to exist between conformers such as the ruffled and saddled structures[13] and is further complicated by the assorted configurations associated with differing solvent interactions and orientations of the 12 phenyl rings. More than one type of structure may be present in the ground state, and the nuclear configuration(s) of the initial ^{1}(d,d) should be sufficiently high in energy that the vibrational relaxation process may be accompanied by a branching into a different distribution of conformers than present in the ground or $^1(\pi,\pi^*)$ states. This difference will be enhanced if the relative zero-point energies of the conformers and the barriers between them differ among the electronic states (Figure 11). Even in the absence of such branching, the vibrational equilibration process per se will correspond to an evolving shift in mean structure if the relevant potential energy surfaces are anharmonic. Such anharmonicity is reasonable considering that out-of-plane deformations are undoubtedly involved in the relaxation processes that occur following photoexcitation of nonplanar porphyrins such as NiDPP.

That significant nuclear motions and perhaps barrier crossings may be involved in the relaxations within the (d,d) excited state of NiDPP is further indicated by the observation that the average time constant of 5−10 ps for the process increases to 20−30 ps as the temperature is reduced from 298 to 200−230 K for NiDPP in methylcyclohexane or toluene (Table 2). There may also be longer components to the overall vibrational/conformational dynamics, especially in mineral oil. This possibility is suggested by the evolution of the absorption between ∼20 and ∼200 ps, which does not appear to involve significant decay of the ground-state bleachings (see Figures 6B, 7C, and 9C). These structural components may also contribute to the wavelength dependence of the time constants, in addition to those occurring on a slightly shorter time scale as the excess vibrational energy is dissipated into the medium.

Decay of the (d,d) Excited State to the Ground State. Previous studies on nominally planar complexes such as NiTPP and NiPPDME have shown that deactivation of the (d,d) state and complete recovery of the ground electronic state is ac-

companied by complete decay of the derivative-like absorption changes with one or more apparent isosbestic points in the spectral collapse.[19−21] This behavior is illustrated in the Soret region for NiPPDME in Figure 10C. A time constant in the range of 250−450 ps at room temperature is typical for these molecules in noncoordinating solvents such as toluene.

Generally similar evolution of the spectrum of the ligand-field excited state is observed in both the Soret and Q regions for NiDPP, in all of the noncoordinating solvents and at all temperatures utilized (see, e.g., Figures 4C, 7D, and 9D). The lifetime of 120−150 ps for the (d,d) state of NiDPP in toluene and methylcyclohexane at 298 K is somewhat shorter than the values observed for the planar complexes. This difference could reflect a slightly improved Franck−Condon factor resulting from a better correspondence between the ^{1}(d,d) to ground state energy gap and coordinate displacement for NiDPP compared to the more planar analogues. Improved Franck−Condon overlap is also thought to contribute to the faster $^1(\pi,\pi^*) \rightarrow$ ground state internal conversion of the nonplanar metal-free porphyrins compared to their planar analogues.[10,11] However, the process appears to be more complex than a simple electronic decay process and probably involves considerable changes in the nuclear coordinates of the porphyrin and perhaps the medium. One indication of such configurational changes is the strong dependence of the decay time on viscosity. The deactivation/recovery time for NiDPP is substantially longer at room temperature in mineral oil, with most of the process occurring with a time constant well over one nanosecond. There also appear to be somewhat faster and slower additional components in mineral oil, which may also be present to some degree in the less viscous media (see Results). The presence of multiple components may derive from several sources, including the vibrational/conformational relaxation/equilibration processes occurring in the ^{1}(d,d) state prior to the change in electronic state, and similar relaxations in the ground electronic state. Furthermore, interconversions among the conformers may be expected to depend on viscosity since the structural changes envisaged involve out-of-plane motions of the macrocycle and concomitant changes in the orientation of the phenyl rings, both of which would involve solvent reorganization.

The increase in the deactivation time as the temperature is reduced from 298 to 200 K in toluene (120 to 350 ps) and from 298 to 200 to 77 K methylcyclohexane (150 ps to 1.7 ns to >3 ns), and the difference in lifetimes between the two solvents at a given temperature, may be due in part to differences in viscosity. The longer lifetimes in both media at low temperature may also reflect the presence of activation barriers between the conformers in the excited and/or ground electronic states.[31] If the temperature dependence of the deactivation/recovery times in toluene or methylcyclohexane is analyzed under this assumption, an activation energy of 2−3 kcal/mol is obtained. This value is consistent with the barrier height estimated to exist between the saddled and ruffled structures of NiDPP in the ground electronic state.[8c] However, our measurements do not permit us to conclude whether the proposed conformational changes and associated barrier crossings accompanying decay of the ligand-field excited state occur in the (d,d) excited state, in the ground state, or both.

Interconversions among the conformational components and differences in electronic relaxation rates among the conformers probably underlie the complexities observed in the spectral evolution accompaning the overall deactivation process. These complexities include subtle readjustments on the 20−200 ps time scale (Figures 7B,C and 9C), multiple kinetic components (Figure 6), and a small increase in the lifetime on the blue edge of the Soret region (Figure 4 inset). These observations and interpretations are fully consistent with the idea that there is a substantial difference in the mean structure of the ^{1}(d,d) and ground electronic states of NiDPP and probably to a lesser degree for NiPPDME and other planar analogues. These structural differences are, again, indicated by the fact that the ^{1}(d,d) and ground-state Soret bands are shifted in different directions for the planar and nonplanar nickel porphyrins (compare Figures 4C and 10C). Overall, we believe that the data as a collective whole are most consistent with the idea that the ^{1}(d,d) $\rightarrow$ ground-state process involves the decay of a ligand-field excited state, having a mean structure with a spread of conformations/configurations populated to varying degrees, to the ground electronic state, having a different mean structure and equilibrium distribution of conformers (Figure 11).

Conclusion

Excitation of nickel(II) porphyrins is followed by a sequence of electronic deactivation steps, $(\pi,\pi^*) \rightarrow$ (d,d) $\rightarrow$ ground state (Figure 11). The deactivation appears to proceed largely in the singlet manifold, although some deactivation through triplet excited states cannot be ruled out. Each change in electronic state appears to be followed by vibrational relaxation and perturbations to the mean structure of the molecule. These electronic, vibrational, and configurational processes are all manifest in the spectra and kinetics. For NiDPP, these processes give rise to complex time evolution of the spectra with components ranging from the subpicosecond time scale for decay of the $^1(\pi,\pi^*)$ state, to several to tens of picoseconds and perhaps longer for vibrational/conformational relaxation in the ^{1}(d,d) excited state, to hundreds of picoseconds to over 1 ns for deactivation of the ^{1}(d,d) state and complete ground-state recovery, depending on solvent and temperature.

The substantial differences in the absorption spectra of both the ground and ligand-field excited states of NiDPP compared to common porphyrins such as NiTPP are readily explained by structural differences between the two porphyrin classes, both before and after photon absorption. The complex spectral evolution and the dependence on solvent, viscosity, and temperature for NiDPP further suggests that each electronic state may have more than one accessible conformer. These conformers may represent saddled or ruffled forms or various combination structures and may also involve the positions and solvent interactions of the 12 phenyl rings.

These results and discussion of NiDPP illustrate the rich photophysics of the nonplanar nickel porphyrins, and the strong interplay between the electronic, conformational, and vibrational properties of these molecules. In future articles we will build upon the framework developed here for NiDPP to discuss other nickel porphyrins that differ in the types and degrees of structural distortions in the ground electronic state, in the rigidity of the macrocycle, and in the electronic effects of the peripheral substituents. The time-resolved studies presented here on NiDPP complement the previous steady-state work on a number of nonplanar porphyrins and the time-resolved studies on several nonplanar metal-free complexes. The collective results demonstrate how dramatically the electronic properties and excited state dynamics of these molecules are modulated by nonplanar distortions and environmental factors. By analogy, our results further illustrate how strongly the functional properties of a porphyrin cofactor can be modulated as a result of the structural and electronic effects imposed by a protein matrix.

Acknowledgment. This work was supported in part by NIH grants GM34865 to D.H. and HL22252 to K.M.S. We thank Drs. David Bocian, Jack Fajer, Steve Gentemann, and John Shelnutt for insightful discussions.

References and Notes

(1) Tetrapyrroles adopt a number of conformations, the most common types being the planar, saddled, and ruffled structures: Scheidt, W. R.; Lee, Y. J. *Struct. Bonding (Berlin)* **1987**, *64*, 1. When in the planar conformation the opposite N−Ni−N angle is ∼180° and the C−N−N−C dihedral is ∼0°. The saddle conformation is characterized by a tilting of alternate pyrrole ring planes above and below the mean plane of the core while the meso carbons remain nearly in the plane (N−Ni−N < 180 and C−N−N−C remains ∼0°) The ruffled conformation is characterized by a twisting of alternate pyrrole ring planes such that the β-pyrrole carbons and meso carbons lie above and below the mean plane of the core (N−Ni−N remains ∼180° and C−N−N−C > 0°).

(2) Harning, T. L.; Fujita, E.; Fajer, J. *J. Am. Chem Soc.* **1986**, *108*, 323. (b) Barkigia, K. M.; Chantranupong, L.; Smith. K. M.; Fajer, J. *J. Am.Chem. Soc.* **1988**, *110*, 7566.

(3) (a) Ladner, R. L.; Heidner, E. J.; Perutz, M. F. *J. Mol. Biol.* **1977**, *114*, 385. (b) Geno, M. K.; Halpern, J. *J. Am. Chem. Soc.* **1987**, *109*, 1238. (c) Deisenhofer, J.; Michel, H. *Science* **1989**, *245*, 1463. (d) Huber, R. *Eur. J. Biochem.* **1990**, *187*, 283. (e) Furenlid, L. R.; Renner, M. W.; Fajer, J. *J. Am. Chem. Soc.* **1990**, *112*, 8987. (f) Alden, R. G.; Ondrias, M. R.; Shelnutt, J. A. *J. Am. Chem. Soc.* **1990**, *112*, 691.

(4) Gunsalus, R. P.; Wolfe, R. S. *Biochem. Biophys. Res. Commun.* **1977**, *76*, 790.

(5) (a) Eschenmoser, A. *Ann. N.Y. Acad. Sci.* **1986**, *471*, 108. (b) Shelnutt, J. A. *J. Phys. Chem.* **1989**, *93*, 6283.

(6) (a) Drain, C. M.; Sable, D.; Corden, B. B. *Inorg. Chem.* **1988**, *27*, 2396. (b) Drain, C. M.; Sable, D.; Corden, B. B. *Inorg. Chem.* **1990**, *29*, 1428.

(7) Ravikanth, M.; Chandashekar, T. K. *Struct. Bond.* **1995**, *82*, 105.

(8) (a) Barkigia, K. M.; Berber, M. D.; Fajer, J.; Medforth, C. J.; Renner, M. W.; and Smith, K. M. *J. Am. Chem. Soc.* **1990**, *112*, 8851. (b) Medforth, C. J.; Senge, M. O.; Smith, K. M.; Sparks, L. D.; Shelnutt, J. A. *J. Am. Chem. Soc.* **1992**, *114*, 9859. (c) Sparks, D. L.; Medforth, C. J.; Park, M.-S.; Chamberlain, J. R.; Ondrias, M. R.; Senge, M. O.; Smith, K. M.; Shelnutt, J. A. *J. Am. Chem. Soc.* **1993**, *115*, 581.

(9) Abbreviations used: TPP, 5,10,15,20-tetraphenylporphyrin; OEP, 2,3,7,8,12,13,17,18-octaethylporphyrin; DPP, 2,3,5,7,8,10,12,13,15,17,18,20-dodecaphenylporphyrin; PPDME, 2,18-dimethylpropionate-3,18-divinyl-3,7,12,17-tetramethylporphyrin; T(*tert*-butyl)P, 5,10,15,20-tetra-*tert*-butylporphyrin; OETPP, 5,10,15,20-tetraphenyl-2,3,7,8,12,13,17,18-octaethylporphyrin.

(10) (a) Takeda, J.; Ohya, T.; Sato, M. *Chem. Phys. Lett.* **1990**, *31*, 5583. (b) Tsuchiya, S. *Chem. Phys. Lett.* **1991**, *183*, 384. (c) Rivikanth, M.; Reddy, D.; Chandrashekar, T. K. *J. Photochem. Photobiol. A: Chem.* **1993**, *72*, 61. (d) Charlesworth, P.; Truscott, T. G.; Kessel, D.; Medforth, C. J.; Smith, K. M. *J. Chem. Soc., Faraday Trans.* **1994**, *90*, 1073.

(11) (a) Gentemann, S.; Medforth, C. J.; Forsyth, T. P.; Nurco, D. J.; Smith, K. M.; Fajer, J.; Holten, D. *J. Am. Chem. Soc.* **1994**, *116*, 7376. (b) Gentemann, S.; Medforth, C. J.; Ema, T.; Nelson, N. Y.; Smith, K. M.; Fajer, J.; Holten, D. *Chem. Phys. Lett.* **1995**, *245*, 441.

(12) (a) Renner, M. W.; Cheng, R.-J.; Chang, C. K.; Fajer, J. *J. Phys. Chem.* **1990**, *94*, 8508. (b) Regev, A.; Galili, T.; Medforth, C. J.; Smith, K. M.; Barkigia, K. M.; Fajer, J.; Levanon, H. *J. Phys. Chem.* **1994**, *98*, 2520. (c) Drain, C. M.; Lehn, J.-M. *J. Chem. Soc., Chem. Commun.* **1994**, 2313. (d) Renner, M. W.; Barkigia, K. M.; Zhang, Y.; Medforth, C. J.; Smith, K. M.; Fajer, J. *J. Am Chem. Soc.* **1994**, *116*, 8582.

(13) (a) Nurco, D. J.; Medforth, C. J.; Forsyth, T. P.; Olmstead, M. M.; Smith, K. M., manuscript in preparation. (b) Caemelbech, E. V.; Forsyth, T. P.; Hobbs, J. D.; Kadish, K. M.; Ma, J.; Medforth, C. J.; Nurco, D. J.; Shelnutt, J. A.; Showalter, M.; Simpson, M. C.; Smith, K. M.; Song, X.; D'Souza, F.; Taylor, K. K., manuscript in preparation.

(14) (a) Alden, R. G.; Crawford, B. A.; Doolen, R.; Ondrias, M. R.; Shelnutt, J. A. *J. Am. Chem. Soc.* **1989**, *111*, 2070. (b) Brennan, T. D.; Scheidt, W. R.; Shelnutt, J. A. *J. Am. Chem. Soc.* **1988**, *110*, 3919. (b) Prendergast, K.; Spiro, T. G. *J. Am. Chem. Soc.* **1992**, *114*, 3793. (c) Cullen, D. L.; Meyer, E. F. *J. Am. Chem. Soc.* **1974**, *96*, 2095. (d) Meyer, E. F. *Acta Crystallogr.* **1972**, *B28*, 2162.

(15) (a) Shelnutt, J. A.; Medforth, C. J.; Berber, M. D.; Barkigia, K. M.; Smith, K. M. *J. Am. Chem. Soc.* **1991**, *113*, 4077. (b) Stichternath, A.; Scheitzer-Stenner, R.; Dreybrodt, W.; Mak, R. S.; Li, X.; Sparks, L. D.; Shelnutt, J. A.; Medforth, C. J.; Smith, K. M. *J. Phys. Chem.* **1993**, *97*, 3701. (c) Barkigia, K. M.; Renner, M. W.; Furenlid, L. R.; Medforth, C. J.; Smith, K. M.; Fajer, J. *J. Am. Chem. Soc.* **1993**, *115*, 3627. (d) Sparks, L. D.; Anderson, K. K.; Medforth, C. J.; Smith, K. M.; Shelnutt, J. A. *Inorg. Chem.* **1994**, *33*, 2297. (e) Hobbs, J. D.; Majumder, S. A.; Luo, L.; Sickelsmith, G. A.; Quirke, J. M. E.;Medforth, C. J.; Smith, K. M.; Shelnutt, J. A. *J. Am. Chem. Soc.* **1994**, *116*, 3261. (f) Jentzen, W.; Simpson, M. C.; Hobbs, J. D.; Song, X.; Ema, T.; Nelson, N. Y.; Medforth, C. J.; Smith, K. M.; Veyrat, M.; Mazzarti, M.; Ramasseul, R; Marchon, J.-C.; Takeuchi, T.; Goddard, W. A., III; Shelnutt, J. A. *J. Am. Chem. Soc.* **1995**, *117*, 11085.

(16) (a) *CRC Handbook of Chemistry and Physics*, 71st ed.; Lide, D. R., Ed.; CRC Press: Boston, 1990. (b) Pauling, L. *The Nature of the Chemical Bond and the Structure of Molecules*, 3rd ed.,; Cornell University Press: Ithaca, NY, 1960.

(17) (a) Antipas, A.; Gouterman, M. *J. Am. Chem. Soc.* **1983**, *105*, 4896. (b) Gouterman, M. In *The Porphyrins*; Dolphin, D., Ed.; Academic Press: New York, 1978; Vol. 3, pp 1−165.

(18) (a) Findsen, E. W.; Shelnutt, J. A.; Ondrias, M. R. *J. Phys. Chem.* **1988**, *92*, 307. (b) Crawford, B. A.; Ondrias, M. R.; Shelnutt, J. A. *J. Phys. Chem.* **1990**, *94*, 6649. (c) Courtney, S. H.; Jedju, T. M.; Freidman, J. M.; Alden, R. G.; Ondrias, M. R. *Chem. Phys. Lett.* **1989**, *164*, 39.

(19) (a) Rodriguez, J.; Holten, D. *J. Chem. Phys.* **1989**, *91*, 3525. (b) Rodriguez, J.; Kirmaier, C.; Holten, D. *J. Am. Chem. Soc.* **1989**, *111*, 6500. (c) Rodriguez, J.; Kirmaier, C.; Holten, D. *J. Chem. Phys.* **1991**, *94*, 6020.

(20) Kobayashi, T.; Straub, K. D.; Rentzepis, P. M. *Photochem. Photobiol.* **1979**, *29*, 925.

(21) (a) Chirvonyi, V. S.; Dzhagarov, B. M.; Timinskii, Y. V.; Gurinovich, G. P. *Chem. Phys. Lett.* **1980**, *70*, 79. (b) Chirvonyi, V. S.; Dzhagarov, B. M.; Shul'ga, M.; Gurinovich, G. P. *Dokl Akad. Nauk. SSSR* **1981**, *259*, 144. (c) Kim, D.; Kirmaier, C.; Holten, D. *Chem. Phys.* **1983**, *75*, 305. (d) Kim, D. H.; Holten, D. *Chem. Phys. Lett.* **1983**, *98*, 584.

(22) (a) Chikisev, A. Y.; Kamalov, V. F.; Korteev N. I.; Kvach, V. V.; Shkvrinov, A. P.; Toluetaev, B. N. *Chem. Phys. Lett.* **1988**, *144*, *90*. (b) Apanasevich, P. A.; Kvach, V. V.; Orlovich, V. A. *J. Raman Spectrosc.* **1989**, *20*, 125. (c) Sato, S.; Kitiagawa, T. *Appl. Phys.* **1994**, *B59*, 415.

(23) (a) Bilsel, O.; Rodriguez, J.; Holten, D. *J. Phys. Chem.* **1990**, *94*, 5945. (b) Rodriguez, J.; Holten, D. *J. Chem. Phys.* **1990**, *92*, 5944. (c) Bilsel, O.; Milam, S. N.; Girolami, G. S.; Suslick, K. S.; Holten, D. *J. Phys. Chem.* **1993**, *97*, 7216.

(24) (a) Seilmeier, A.; Scherer, P. O. J.; Kaiser, W. *Chem. Phys. Lett.* **1984**, *105*, 140. (b) Hill, J. R.; Chronister, E. L.; Chang, T.-C.; Kim, H.; Postlewaite, J.-C.; Dlott, D. D. *J. Chem. Phys.* **1988**, *88*, 949. (c) Sukowski, U.; Seilmeier, A.; Elaesser, T.; Fischer, S. F. *J. Chem. Phys.* **1990**, *93*, 4094. (d) Sension, R. J.; Szarka, A. Z.; Hochstrasser, R. M. *J. Chem. Phys.* **1992**, *97*, 5239.

(25) Kadish, K. M.; Franzen, M. M.; Han, B. C.; Araullo-McAdams, C.; Sazou, D. *J. Am. Chem. Soc.* **1991**, *113*, 512.

(26) Several observations suggest that the expected Soret absorption of the $^1(\pi,\pi^*)$ state may be only slightly red-shifted from a somewhat stronger ground-state Soret band for the nickel porphyrins and cancellation of the two prevents direct observation of the former. These observations are (i) the (π,π^*) Soret absorption has a variable intensity (and position) relative to the bleaching in the transient difference spectra previously observed for metalloporphyrins, ranging from about 50% in zinc(II) porphyrins to about 20% in copper(II) porphyrins,[19b] (ii) the maximal bleaching in the $^1(\pi,\pi^*)$ spectrum of NiDPP occurs about 5 nm to shorter wavelengths than the position of the ground-state Soret band (Figures 3 and 4A), and (iii) the amplitude of the bleaching is about 40% of that expected based on the amplitudes of the bleachings in the Q bands.

(27) Drain, C. M.; Nurco, D. J.; Medforth, C. J.; Smith, K. M.; Holten, D., manuscript in preparation.

(28) At first glance, the data in the Soret region in Figure 4A seem to contradict the Q-band data and suggest that substantial ground-state recovery occurs during the $^1(\pi,\pi^*)$ lifetime. However, closer examination of these data and the spectra at longer times attributed to the (d,d) excited state (Figure 4B) suggest a different interpretation. The apparent bleaching decay occurring during the first picosecond after excitation probably arises from a blue-shift (and perhaps increased strength) of the excited-state Soret band compared to the $^1(\pi,\pi^*)$ spectrum such that increasing cancellation of the bleaching occurs over this period. This scenario is indicated by (i) the arguments presented above[26] that a Soret absorption of the $^1(\pi,\pi^*)$ state is expected and that its position is slightly to the red of the ground-state Soret band and thus significantly overlaps the Soret bleaching and (ii) the observation that, as the $^1(\pi,\pi^*)$ state decays and the (d,d) state forms, the decreasing bleaching amplitude is accompanied by a red-shift in the position of the bleaching and by the growth of a positive absorption to the blue (Figure 4A). Hence, the data in the Soret region are consistent with the more straightforward conclusion drawn from the data in the Q-band region that ground-state recovery reflects only a small (<30%) fraction of the $^1(\pi,\pi^*)$ decay.

(29) Since similar spectra of the ligand-field excited state have been observed for NiTPP, NiOEP, NiPPDME, and all the other nickel porphyrins investigated previously, specific effects involving the peripheral groups appear to be relatively unimportant. Since similar results have been found for all of these molecules using several different excitation wavelengths, it is unlikely that the red-shifts derive from excitation of some fraction of slightly distorted molecules that may be present in solution.

(30) Drain, C. M.; Nurco, D. J.; Ema, T.; Nelson, N. Y.; Medforth, C. J.; Smith, K. M.; Simpson, C.; Shelnutt, J. A.; Holten, D., manuscript in preparation.

(31) Such barriers probably do not reflect a requirement that the ^{1}(d,d) excited state thermally repopulate a higher energy electronic state, since other (d,d) states such as $(d_\pi,d_{x^2-y^2})$ should not have substantially different inherent decay times, and other short-lived excited states such as metal ↔ ring charge-transfer states should be at considerably higher energy.

JP960735J